P11.142

OPERATIONAL RAINFALL ESTIMATION BY X-BAND MP RADAR NETWORK IN MLIT, JAPAN

Takeshi Maesaka*, Masayuki Maki and Koyuru Iwanami
National Research Institute for Earth Science and Disaster Prevention, Tsukuba, Ibaraki, Japan
Shuichi Tsuchiya
National Institute for Land and Infrastructure Management, Tsukuba, Ibaraki, Japan
Kaori Kieda and Ayumi Hoshi
Advanced Engineering Services, Tsukuba, Ibaraki, Japan

1. INTRODUCTION

National Research Institute for Earth Science and Disaster Prevention (NIED) deployed X-band multi-parameter (MP) radars around the Tokyo metropolitan area in 2000 and 2008, and has studied on quantitive precipitation estimation (QPE) and the radar network since then (Maki *et al.* 2005a and b; Park *et al.* 2005a and b; Maki *et al.* 2010). When flood disasters caused by localized heavy rainfall frequently occurred in Japan in July and August 2008, NIED succeeded in a real-time monitoring of the heavy rainfalls with K_{DP}–R relationship. The NIED's results boosted Ministry of Land, Infrastructure, Transport and Tourism (MLIT) to start deploying the X-band MP radars in Japan. MLIT deployed 26 radars in four great urban areas (Tokyo, Nagoya, Kinki and Fukuoka) and local major cities in FYs 2009 and 2010 (Fig. 1). NIED developed an operational data processing system, which estimates the rainfall intensity from the radar data, and which creates regional composite data every one minute, under a commission from National Institute for Land and Infrastructure Management (NILIM), MLIT. The system has experimentally been operated since July 2010, and provides the rainfall information which is updated every one minute via the Internet.

This paper describes on i) specifications of MLIT X-band MP radars, and ii) the operational data processing to estimate a distribution of rainfall intensity using MLIT MP radar data.

2. MLIT X-BAND MP RADAR NETWORK

In recent years, it has been pointed out that urban area implies a vulnerability to localized heavy rainfall. So high accurate, space- and time-resolving QPE is expected for a water management in the urban cities. As we know, QPE using X-band polarimetric parameters has a good accuracy comparable to the rain gauge observation. This means that rapid QPE is possible because it does not need a calibration by the rain gauge. Moreover, the beam width of X-band radar does not become wider than C- or S-band radars, because the observation range of X-band is generally shorter than those of C- and S- band radars. According to these reasons, X-band MP radar seems to be suitable for the urban water management; however it has a big disadvantage: a rain attenuation. So MLIT deployed the radars with the following policies.

- Designating an intensive observation area (IOA), such as densely inhabited districts, landslide areas, and volcanoes.
- Covering the IOA by several radars to compensate the rain attenuation by each other radar.
- The distance between each radar should be about 40 km.
- Each radar should cover the IOA within the range of about 30 km (high space-resolving area with narrow beam width).
- A few beam blocking by terrains or artificial objects.

Figure 1 shows the radar distributions and their observation ranges of MLIT X-band MP radar network. Each radar belongs to a particular area where the designated IOA is. By compositing the estimated rainfall intensities of the radars which belong to the same area, final QPE product (meshed rainfall intensity data) is created in each area.

Table 1 shows typical specifications of MLIT X-band MP radar, though several manufacturers supplied a variety of radar systems to MLIT. Almost all the radars which were supplied in FY

* *Corresponding author address:* Takeshi Maesaka, National Research Institute for Earth Science and Disaster Prevention, 3–1 Tennodai, Tsukuba, Ibaraki, 305–0006, Japan. e-mail: maesaka@bosai.go.jp

Figure 1: Radar distributions and their coverages of MLIT X-band MP radar network. Triangles indicate the radar locations. Circles indicate the observation ranges (r = 80 km). Capital and bold letters indicate the area names. Each radar belongs to a particular area; the radar (triangle and circle) with the same color as the capital and bold letters belongs to the area.

2009 use a klystron as a microwave amplifier; however solid state devices were mostly used in FY 2010.

In each radar site, the observed radar data, which are separated tilt-by-tilt, are converted to MLIT data format, and the converted data are immediately transferred to two data processing centers in Kanto and Kinki Regional Development Bureaus, MLIT. The same processing is performed for redundancy in these two centers.

3. DATA PROCESSING

In this section, it is described how the input observation data are processed to create the areal distribution of rainfall intensity in the data processing centers. Although some threshold value described below can be customized for each radar site, we denote the typical values here.

3.1 *Quality Control (Initial)*

First of all, the following quality controls are applied to eliminate noises, ground clutters, and non-meteorological echoes from the input data.

a. *Masking area*

The range bin data in blanking zones or known clutter areas are eliminated by a masking map (geographical polygons) prepared in advance.

b. *Close range*

The range bin data within 1 km from the radar are eliminated.

c. *Low SNR*

The range bin data whose SNR is less than 3 dB are eliminated. Note that this elimination has already been processed at the radar site, currently. These data are handled as “no rain”.

d. *Calibration of received power (Pr)*

Pre-determined offsets of horizontal and vertical received powers are added to Pr_{h} and Pr_{v}, respectively.

Table 1: Specifications of MLIT X-band MP radar.

Features	Specifications
Microwave amp.	Klystron or solid state device
Frequency	9700 MHz – 9800 MHz
Transmit power	100 kW ^{*1}
Pulse width	1.0 μ sec. ^{*2}
Occu. bandwidth	$\leq$ 4 MHz
Pulse Rep. Freq.	1200 Hz – 1800 Hz ^{*3}
Antenna	Parabola, $\phi \leq$ 2.2 m
Antenna gain	$\geq$ 42 dBi
Beam width	$\leq$ 1.2 $^\circ$
Polarization	H & V, Simultaneous transmit/receive
Min. Sensitivity	$\leq$ -110 dBm
Observation range	80 km
Data resolution	150 m (range) 1.2 $^\circ$(azimuth)
Sampling number	100 (approximately, at PRF=1800 Hz)
Output parameters	$Pr_{\text{H,nor}}$, $Pr_{\text{V,nor}}$, $Pr_{\text{H,mti}}$, $Pr_{\text{V,mti}}$, V, W, Φ_{DP}, $\rho_{\text{HV}}{}^{*4}$

*1. This transmit power is equally divided to H/V. If the solid state device is used, this power includes the pulse compression gain. In Shizuoka area, the transmit power is 50 kW.
*2. If the solid state device is used, this value is pulse-compressed.
*3. Dual-PRF observation is available.
*4. Subscriptions H and V for Pr (received power) indicate the polarizations. Subscriptions mti and nor also indicate that clutter removal by coherent motion target inhibition is applied or not.

e. *Ground clutter removal*

The Φ_{DP} and ρ_{HV} are eliminated if the difference between $Pr_{\text{H,nor}}$ and $Pr_{\text{H,mti}}$ is larger than 5 dB. Because this removal may underestimate the reflectivity at the range bins where the Doppler velocity is almost zero, these range bins within 15 km from the radar are handled as “no data”. These areas should be compensated by other radars.

f. *Unfolding of Φ_{DP}*

In case Φ_{DP} exceeds 360 deg, Φ_{DP} is unfolded with a consideration of the continuity.

g. *Texture parameter of Φ_{DP}*

The Φ_{DP} and ρ_{HV} are eliminated if texture parameter of Φ_{DP}, which is a difference from the running average, is larger than 10 $^\circ$.

h. *Threshold of ρ_{HV}*

The Φ_{DP} and ρ_{HV} are eliminated if the ρ_{HV} is less than 0.6.

i. *Beam blocking*

A beam blocking rate data with the coordinates of elevation, azimuth and range have been created for each radar site by using a digital elevation map (DEM) with the horizontal resolution of 50 m. The Pr data are corrected by multiplication of the interpolated blocking rate. If the interpolated blocking rate is larger than 50 %, the range bin data are eliminated.

j. *Point clutter*

The range bin data are eliminated, if the texture parameter ofPr is larger than 20 dB.

3.2 Estimation of K_{DP}

K_{DP} is the most important polarimetric parameter for rainfall estimation using X-band MP radar. The K_{DP} is calculated by a differentiation of Φ_{DP}; however the observed Φ_{DP} is usually contaminated by noises and differential scattering phase. This is why the observed Φ_{DP} should be space-filtered, but the filtering may make the spacial resolution coarse, or may make the K_{DP} underestimated in heavy rainfall area. So two types of finite impulse response (FIR) filters and adaptive window of linear regression are used in the MLIT system.

a. *Filtering of Φ_{DP}*

FIR filters with long and short cutoff lengths are applied before the differentiation of Φ_{DP}. At first, the long filter is applied to remove the differential scattering phase in strong reflectivity area. This method was proposed by Hubbert and Bringi (1995), and almost the same procedure is used in the MLIT system. The cutoff length of the long FIR filter is 4.0 km. Then the short filter whose cutoff length is 2.0 km, is applied to smooth the Φ_{DP}.

b. *Linear regression (Tentative)*

For the differentiation of Φ_{DP}, gradients of Φ_{DP} are calculated by linear regression. When the gradient at one range bin (bin index = i) is calculated, the neighbor 30 range bins (from bin$_{i-15}$ to bin$_{i+15}$) are tentatively used as the window of linear regression. The tentative K_{DP} is calculated by dividing the gradient by 2.

c. *Linear regression (Adaptive)*

Some Φ_{DP} fluctuations with the wave length of several kilometers sometimes remain in the filtered Φ_{DP} series along the ray. These fluctuations cause repetitions of positive and negative K_{DP} along the ray, although K_{DP} should be positive value in pure rainfall (not including ice phases). The needless negative K_{DP} can be suppressed by making the window of linear regression wider, but this also makes the peak value of K_{DP} smaller. Because these fluctuations usually occur in weak rain region, we make the window width varying inversely as tentative K_{DP} which has a relation to rainfall intensity. That is to say, narrow (wide) window width is used to calculate the finale K_{DP} in heavy (weak) rainfall region, respectively.

Figure 2 shows the adaptive relationship between the tentative K_{DP} and the window width used in the MLIT system. The linear regressions are performed once again with the adaptive window width to calculate the final K_{DP}.

3.3 *Attenuation Correction (Tentative)*

Attenuation by rainfall is not negligible in X-band weather radar, so the correction is necessary for the rainfall monitoring. We estimate the attenuation of the horizontal polarization per unit length (A_{h} [dB km^{-1}]) from the K_{DP} using the following equations.

$$\begin{aligned} A_{\mathrm{h}} &= a_1 K_{\mathrm{DP}}^{b_1}, \qquad (1)\\ a_1 &= 0.2925 + 7\times10^{-4} el \\ &\quad +1\times10^{-5} el^2 + 3\times10^{-6} el^3, \\ b_1 &= 1.1009 - 3\times10^{-5} el \\ &\quad -4\times10^{-6} el^2, \end{aligned}$$

where el is a radar beam elevation angle ($^\circ$). This relationship is based on the scattering simulation

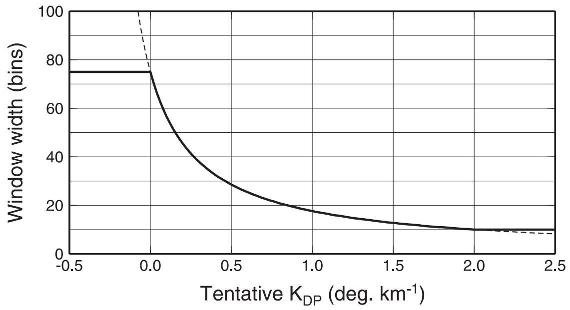

Figure 2: Relationship between the tentative K_{DP} and the window width. Maximum and minimum numbers of the window width are 75 and 10, respectively. The inverse proportional function (broken line) goes through the points (K_{DP},width) = (0.0, 75) and (2.0, 10).

in Park *et al.* (2005a), and it is approximated with a consideration of the elevation dependency. Tentative horizontal reflectivity (Z_{h}), which is calculated from $Pr_{\mathrm{h,mti}}$ according to the radar equation, is corrected by adding the range-integrated A_{h}. This tentative Z_{h} is used for next quality control of K_{DP}.

3.4 *Quality Control (K_{DP})*

In weak rainfall region, it is difficult to estimate the rainfall intensity from the K_{DP}, because the estimation accuracy of the K_{DP} is not enough. Moreover, the repetitions of positive and negative K_{DP}, as described in Section 3.2.c, may still remain in the weak rainfall region. So when the Z_{h} is less than 30 dBZ, the K_{DP} is eliminated.

3.5 *Attenuation Correction (Final)*

Using the quality-controlled K_{DP}, the attenuation correction is performed again in the same manner as Section 3.3. Furthermore the attenuation of differential reflectivity (Z_{DR}), which is calculated as $Pr_{\mathrm{h,mti}}/Pr_{\mathrm{v,mti}}$, is also corrected by using following equation.

$$\begin{aligned} A_{\mathrm{DR}} &= a_2 K_{\mathrm{DP}}^{b_2}, \qquad (2)\\ a_2 &= 0.0298 + 5\times10^{-6} el \\ &\quad +2\times10^{-6} el^2 + 3\times10^{-8} el^3, \\ b_2 &= 1.293, \end{aligned}$$

where A_{DR} is a attenuation of the differential reflectivity per unit length [dB km^{-1}].

3.6 *Quality Control (by Z_{DR})*

For removing non-meteorological echo, the range bin data whose Z_{DR} exceeds predetermined range (for example, -2 dB – 6 dB) are eliminated. Note that this quality control is not performed at present, because the Z_{DR} offset (the difference between the horizontal and vertical received power offsets) has not been determined yet.

3.7 *Radio Wave Extinction Area*

X-band weather radar sometimes misses precipitation echoes behind heavy rainfall by the rain attenuation. We cannot know if there is a rainfall or not in this radio wave extinction area. When the distribution of rainfall intensity is graphically drawn, this area should be shown not as "no rain" area but as unknown area where it may be rain. The detection of this area is performed by Iwanami *et al.* (2007).

The radio wave extinction area is where a distance from the radar (r) satisfies the following equation,

$$2 \times PIA(r) \geq dBZ_{\text{thresh}} - dBZ_0(r), \qquad (3)$$

where $dBZ_0(r)$ is the minimum detectable reflectivity at r, dBZ_{thresh} is a detection threshold of reflectivity, and $PIA(r)$ is a path integrated attenuation (one way). The $PIA(r)$ is calculated as,

$$PIA(r) = \int_0^r A_{\text{h}}(r)dr. \qquad (4)$$

The detection threshold is set as the reflectivity corresponding to 3 mm hour^{-1} rainfall (according to Z–R relationship). If the K_{DP} is available in the extinction area, the K_{DP} is used for rainfall estimation.

3.8 *Estimation of Rainfall Intensity*

The estimation of rainfall intensity is performed by the following flow.

a. K_{DP}–R relationship

If K_{DP} is available below melting layer, the rainfall intensity is calculated as,

$$\begin{aligned} R &= c \times a_3 K_{\text{DP}}^{b_3}, \qquad (5)\\ a_3 &= 19.6 + 2.71 \times 10^{-2} el \\ &\quad +1.68 \times 10^{-3} el^2 + 1.11 \times 10^{-4} el^3, \\ b_3 &= 0.815, \end{aligned}$$

where c is a calibration factor. This relationship is also based on Park *et al.* (2005a). The calibration factor, which has been determined by the comparison with the rain gauge observation, is 1.3 at present.

The top height of the melting layer is determined by the 0 °C level of operational mesoscale simulation by Japan Meteorological Agency, and the thickness of the layer is assumed as 1 km.

b. Z–R relationship

Then, Z–R relationship is used to estimate the rainfall intensity, if the Z_{h} is available. The relationship for rain (snow) is used below (above) the melting layer, respectively, and these are individually determined for each radar site. In the melting layer, mixed relationship, which transits linearly between rain and snow, is used for avoiding the estimation gap.

3.9 *Interpolating and Compositing*

The estimated rainfall intensities of each radar site are interpolated and composited into the geographical grid mesh with the resolutions of longitudinal 45/4 ° and latitudinal 30/4 ° (250 m, approximately). The modified Cressman interpolation is used in this process.

A sampling radius R_{s} [m] is defined as a linear function of the distance from the radar (r),

$$R_{\text{s}} = a_4 r + b_4, \qquad (6)$$

for considering the radar beam spreading. Now a_4 and b_4 are set as 0.013 and 150 m, respectively.

A Weighting function of the Cressman interpolation (W) is defined as,

$$\begin{aligned} W &= w_{\text{h}} \times w_{\text{a}}, \qquad (7)\\ w_{\text{h}} &= \frac{1}{1 + C_{\text{h}} \left(\frac{d}{R_{\text{s}}}\right)^2}, \qquad (8)\\ w_{\text{a}} &= \frac{1}{1 + C_{\text{a}} \left(\frac{h}{H}\right)^2}. \qquad (9) \end{aligned}$$

w_{h} is a horizontal weighting, d is a distance between the grid point and range bin, and C_{h} is a control coefficient of w_{h}. When the range bin is out of the sampling circle ($d > R_{\text{s}}$), the bin is not sampled ($w_{\text{h}} = 0$). w_{a} is an altitudinal weighting, h is a altitude above ground level, C_{a} is a control coefficient of w_{a}, and H is a maximum interpolation height. When the bin altitude h is higher than H, the bin is not sampled ($w_{\text{a}} = 0$). w_{a} is introduced because lower altitude observation is more correlative with the ground level rainfall as long as ground clutters and non-meteorological echoes are removed by the appropriate quality control. Now C_{h}, C_{a}, and H set as 0.5, 20.0 and 5000 m, respectively.

Then 3×3 median filter is performed to the interpolated mesh data for smoothing. Finally, gap grids, which are not interpolated by the available data, are filled by 5×5 Gaussian filter.

Figure 3 shows the example Plan Position Indicators (PPIs) of the rainfall intensities estimated by this MLIT system. At the time, a rain band accompanied by Typhoon 1112 (Talas) went through Nagoya area. Because the maximum intensity of this rain band was about 100 mm hour^{-1}, many radio wave extinction areas were detected (gray shades in Fig. 3).

Figure 4 shows the areal composite of the estimated rainfall intensity in Nagoya area. The estimated intensities of the radar shown in Fig. 3 were used to create this composite. Two PPIs with different elevation angle are used for each radar. The radio wave extinction area was compensated by other radars in the overlapped observation area.

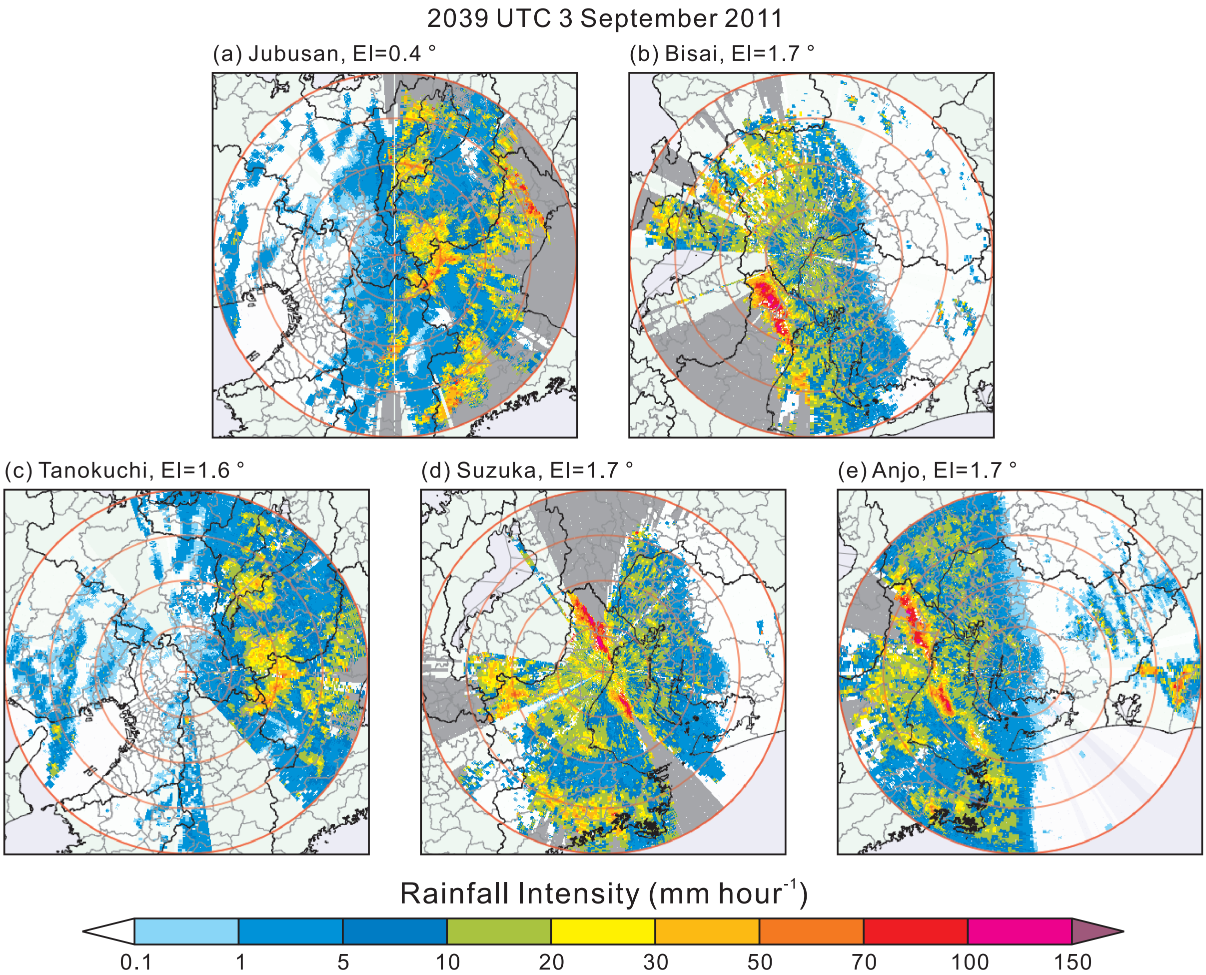

Figure 3: PPIs of the estimated rainfall intensity at 2039 UTC 3 September 2011. a) Jubusan radar, b) Bisai radar, c) Tanokuchi radar, d) Suzuka radar and e) Anjo radar. Gray shade indicates the radio wave extinction area. Range circles are drawn every 20 km by red lines.

4. CONCLUSION

The precipitation information calculated by this system is experimentally provided by MLIT since July 2010. The minutely updated rainfall intensity is now browsable in web site,

“http://www.river.go.jp/xbandradar/”.

(Unfortunately, there is no English page at present. Please click the area shown in a top page map.) The accurate information updated every minute is sure to contribute to the monitoring of extreme weather in urban areas.

Acknowledgment

The national project, development of the X-band MP radar network, was planned and carried out by constructive, dedicated and patient members of River Information Policy Planning Office, River Planning Division, Water and Disaster Management Bureau, and Electricity and Telecommunication Office, Engineering Affairs Division, Minister’s Secretariat in Ministry of Land, Infrastructure, Transport and Tourism, Japan. This project succeeded under the comprehensive cooperation by bureaucrats, radar manufacturers, consultants and research institutes. We would like to express our gratitude to all members concerned with this project. We are proud that we participated in this fruitful project.

References

Iwanami, K., T. Maesaka, K. Kieda, M. Maki, R. Misumi, and S. Shimizu, 2007, Simple attenuation correction method in rainfall observation with X-band polarimetric radar. *Proc. of 2007 Spring Meeting of Meteor. Soc. of*

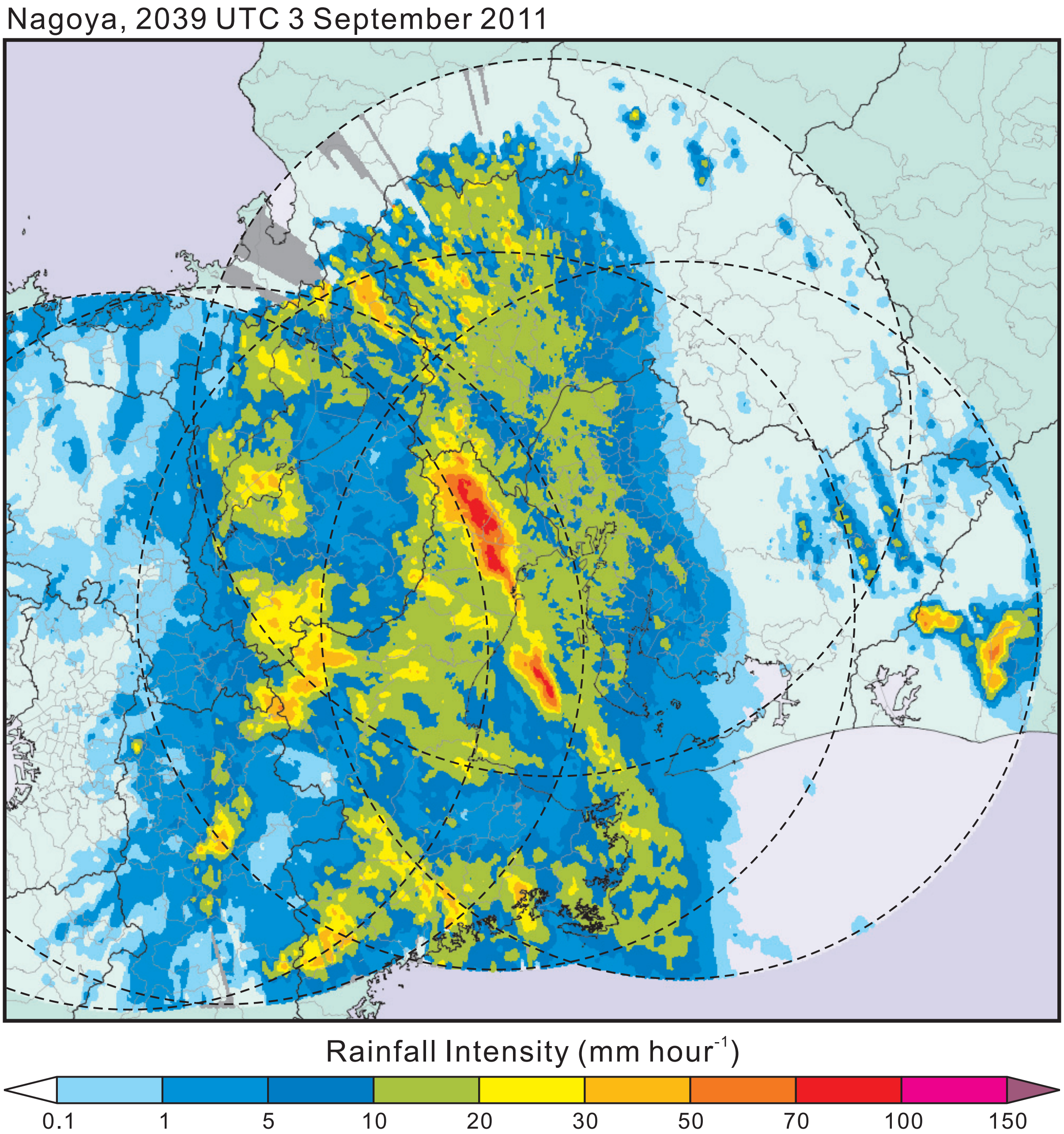

Figure 4: Areal composite of the estimated rainfall intensity in Nagoya area at 2039 UTC 3 September 2011. Broken circles are the observation ranges of the radars used to create this composite. Gray shade indicates the radio wave extinction area.

Japan., B463 (in Japanese).

Hubbert, J. and V. N. Bringi, 1995, An interactive filtering technique for the analysis of copolar differential phase and dual-frequency radar measurements. *J.Atmos. Oceanic Technol.*, **12**, 643–648.

Maki, M., S.-G. Park and V.N. Bringi, 2005a, Effect of natural variations in rain drop size distributions on rain rate estimators of 3 cm wavelength polarimetric radar, *J. Meteor. Soc. Japan*, **83**, 871–893.

———, K. Iwanami, R. Misumi, S.-G. Park, H. Moriwaki, K. Maruyama, I. Watabe, D.-I. Lee, M. Jang, H.-K. Kim, V.N. Bringi, and H. Uyeda, 2005b, Semi-operational rainfall observations with X-band multi-parameter radar, *Atmos. Sci. Letters*, **6**, 12–18.

———, T. Maesaka, A. Kato, S. Shimizu, D.-S.

Kim, K. Iwanami, S. Tsuchiya, T. Kato, Y. Kikumori, and K. Kieda, 2010, X-band polarimetric radar networks in urban areas, *Proc. of 6th Europian Conf. on Radar in Meteor. and Hydrol.*, P15.10.

Park, S.-G., V.N. Bringi, V. Chandrasekar, M. Maki and K. Iwanami, 2005, Correction of radar reflectivity and differential reflectivity for rain attenuation at X-band wavelength. Part I: Theoretical and Empirical Basis, *J. Atmos. Oceanic Technol.*, **22**, 1621–1632.

———, M. Maki, K. Iwanami, V.N. Bringi, and V. Chandrasekar, 2005, Correction of radar reflectivity and differential reflectivity for rain attenuation at X-band wavelength. Part II: Evaluation and application., *J. Atmos. Oceanic Technol.*, **22**, 1633–1655.